IUPAC International Union of Pure and Applied Chemistry

REPRINTED FROM

Molecular Electronics

A 'Chemistry for the 21st Century' Monograph

ISBN 0-632-04284-2

EDITED BY

J. JORTNER & M. RATNER

Blackwell
Science

11 Micro- and Nanofabrication Techniques Based on Self-assembled Monolayers

P.F. NEALEY*, A.J. BLACK†, J.L. WILBUR† and G.M. WHITESIDES†

*Department of Chemical Engineering, University of Wisconsin-Madison, 1415 Johnson Dr., Madison, WI 53706, USA

†Department of Chemistry, Harvard University, Cambridge, MA 02138, USA

1 Introduction

New fabrication techniques are required to continue the trend in the microelectronics industry to work at smaller scale. Optical lithography [1], the most widespread technique for the fabrication of microelectronic devices, is approaching the lower limit (~100 nm) in the size of features that it can produce. Smaller features (50 nm) can be produced with electron beam writing or atom-by-atom manipulation. These processes, however, are currently linear and will require significant development for high-volume commercial applications. Opportunities exist to develop fabrication techniques that are based on different principles to reach the scale of 50 nm. Desirable attributes of any new fabrication technique include low cost (capital and operational), low environmental impact, and the ability to make complex structures of appropriate scale reproducibly with low levels of defects.

Molecular- or atomic-scale devices based on the electronic properties of single molecules represent a plausible lower limit in size. Efforts to fabricate these devices have defined the emerging field of molecular electronics. Even if useful devices of scale 1–30 nm can be synthesized, however, a host of problems present themselves for the application of the molecular-scale devices. Structures between 100 nm and 1 nm will still be needed, for example, to make internal and external interconnects, or for use in new architectures such as cellular automata to access the molecular-scale devices.

Molecular self-assembly is a potential strategy for fabrication of structures with dimensions that range from nanometres to millimetres [2,3]. In molecular self-assembly, subunits of molecular dimensions, whose structures can be controlled with atomic resolution, spontaneously form molecularly ordered aggregates [4,5] with certain dimensions of 1–100 nm. Self-assembly leads to equilibrium structures that are at (or close to) thermodynamic minimum [6,7], and result from multiple, weak, reversible interactions such as hydrogen bonds, ionic bonds, and van der Waals forces between subunits. The information that determines the final structure of the aggregate is coded in the structure and properties of the subunits. As a strategy for fabrication, self-assembly is thus automatically defect rejecting [5], and self-registering on a scale that is too small for current techniques for microfabrication and too large for conventional organic synthesis. The principles of self-assembly are observed in nature [4–6,8,9]; processes such as protein folding and aggregation [10] and formation of DNA double helices [11] serve as biological models for the potential of self-assembly in microfabrication. Table 11.1 shows some examples of self-assembling systems.

Self-assembled monolayers (SAMs) represent the most widely studied and best developed class of non-biological self-assembling systems. SAMs are highly ordered

Table 11.1 Self-assembling systems.

System	Smallest dimension	Refs
Self-assembled monolayers	1–2 nm	[12–18]
Langmuir–Blodgett films	1–2 nm	[14,15]
Liquid crystals	1 nm	[19]
Hydrogen-bonded aggregates	1.5 nm	[20]
Templated crystals	0.1 nm	[21,22]
Block copolymers	1–2 nm	[23]
Systems in nature	1 nm	[4–6,8–11]

molecular assemblies of long-chain alkanes that chemisorb on the surfaces of appropriate solid materials. The structure of SAMs, effectively two-dimensional crystals with controllable chemical functionality, makes them ideal model systems for the investigation of wetting, adhesion, lubrication, corrosion, protein adsorption, and cell attachment [12–18].

This chapter describes the principles, achievements, and potential of micro- and nanofabrication techniques that are based on self-assembled monolayers; the systems that are discussed have at least one dimension of molecular scale. We have demonstrated applications for SAMs in microelectronics that include passivation of surfaces, use of SAMs for ultrathin resists and masks, directed deposition of materials on surfaces patterned with SAMs, and the use of chemical and biochemical functionality on the surface of SAMs for sensors.

2 Self-assembled monolayers

2.1 *Alkanethiols on gold*

Self-assembled monolayers of alkanethiolates on gold (RSH/Au) are the best studied system of self-assembled monolayers [24,25]. The RSH/Au system is attractive because of: (i) ease of fabrication; (ii) degree of perfection; (iii) chemical stability under ambient laboratory conditions; (iv) availability of materials; and (v) flexibility in chemical — and thus surface — functionality. Two important factors may limit the use of current hydrocarbon-based SAMs of alkanethiolates on gold in microelectronic devices: (i) they are thermally unstable above 100°C [26] and (ii) the high rate of diffusion of gold into Si; this property makes gold structures on silicon largely incompatible with current techniques of microfabrication [27]. SAMs of alkanethiolates on gold, however, can serve as models or prototypes for new techniques or applications that will be generally applicable to new classes of SAMs designed specifically for microprocessing and microfabrication.

2.1.1 PREPARATION AND GENERAL STRUCTURE

Self-assembled monolayers of alkanethiolates on gold form by spontaneous adsorption of alkanethiols [$X(CH_2)_nSH$] [12–18,25,28–33] or dialkyldisulfides [$X(CH_2)_nS\text{–}S(CH_2)_mY$] [33,34] onto gold, either from solution or the vapour phase (Eqn 11.1).

$$\text{X-R-SH} + \text{Au(0)}_n \rightarrow \text{X-R-S}^- \text{Au(I)} \cdot \text{Au(0)}_n + 1/2\text{H}_2 \quad (11.1)$$

$$1/2\,(\text{X-R-S})_2 + \text{Au(0)}_n \rightarrow \text{X-R-S}^- \text{Au(I)} \cdot \text{Au(0)}_n.$$

Dialkylsulfides [$X(CH_2)_nS(CH_2)_mY$] also form SAMs [35], but are significantly less reactive than alkanethiols, and form SAMs of poorer quality. Assembly of thiolates may also be induced by electrochemical oxidation of alkanethiols in solution [36] using gold as an electrode. Thiols are generally preferred over disulphides and sulphides for the preparation of SAMs because they are more soluble, react with the surface of the gold $\sim 10^3$ faster [33,37], and yield monolayers of better quality. In addition, they are easier to synthesize (many are available commercially).

Typically, thin (20–50 nm) films of gold are used as substrates for SAMs; SAMs also form on colloidal gold [38–40]. The gold films are usually deposited by electron beam or thermal evaporation onto a solid, flat support such as a polished silicon wafer (with a native oxide), a sheet of mica, or a glass slide. Because gold does not wet these surfaces, an adhesion promoter such as titanium, chromium, or an appropriate organic material [41,42] is used.

2.1.2 STRUCTURE AT THE ATOMIC SCALE

The mechanistic details [32] of the reaction of thiols or disulphides with the gold surface are not completely understood. The fate of the hydrogen atom in the case of alkanethiol adsorption, for example, and the exact structure of the resulting monolayer are not known [43]. On Au(111) the sulphur atoms are thought to form an overlayer commensurate with the Au atoms with structure $(\sqrt{3} \times \sqrt{3})R30°$. Recent X-ray diffraction studies, however, suggested that the species on the surface is a disulphide [44] (rather than a thiolate [15,16]). The alkyl chains extend perpendicularly from the plane of the surface in a nearly all-*trans* configuration. To maximize the van der Waals interactions between adjacent methylene groups ($\sim$1.5–2 kcal mol^{-1} per CH_2) [15,16], the chains tilt at an angle of 30° with respect to the surface normal (Figure 11.1(a)). These van der Waals forces ($\sim$20–30 kcal mol^{-1} for $C_{16}SH$) and the strength of the sulphur–gold bond ($\sim$44 kcal mol^{-1}) drive formation of the monolayer. The resulting structure on the atomic scale is ordered: for alkyl chains with $n > 6$, the monolayer is quasi-crystalline in two dimensions. Table 11.2 summarizes the characterization of SAMs of alkanethiols on gold.

2.1.3 DEFECTS

Figure 11.1(b) shows high resolution scanning tunnelling microscopy (STM) images (from Delamarche *et al.* [63,64]) of dodecanethiol adsorbed on Au(111). The sample in the large image was annealed at 100°C for 10 h in air. A step in the gold surface runs from the upper right corner to the centre of the image where it disappears with a screw dislocation. The occassional black lines that parallel it are depressions in the monolayer where neighbouring thiols have either tilted over or migrated to cover missing lines of thiols. Although molecular resolution is apparent, the c(4*2) rectangular superlattice structure is not clearly discernible because of the large scan size. The inset shows a similar sample that was not annealed. The gold terrace has five depressions: these are

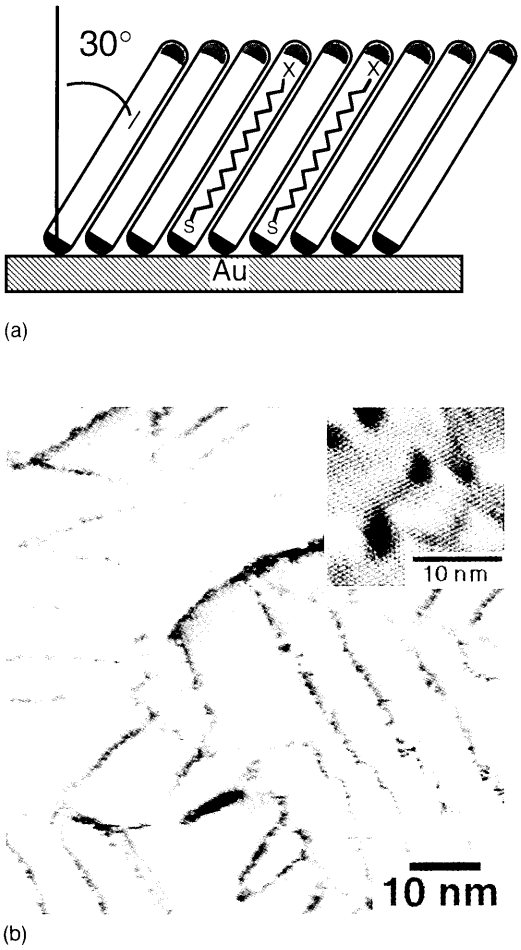

Figure 11.1 (a) Schematic illustration of the molecular-level structure of a self-assembled monolayer of *n*-alkanethiolates on gold. Modification of the head group, X, allows control of the monolayer's surface properties, and the thickness of the monolayer depends on the length of the alkyl chain. (b) Scanning tunnelling micrograph of dodecanethiol adsorbed on Au(111) that shows a gold step, a screw dislocation in the centre, and depressed lines in the monolayer due to the accommodation of missing lines of thiols by vicinal molecules. The inset shows five depressions (gold pits 2.4 A deep) in the centre that are linked by domain boundaries. The monolayer packing corresponds to a phase of the c(4*2) rectangular superlattice. These images were provided by Delamarche *et al.* [63]. See text for references.

Table 11.2 Properties of self-assembled monolayers of thiols on gold.

Monolayer property	Technique	Refs
Structure	Surface Raman scattering	[45]
	Transmission (high energy) electron diffraction	[46]
	Low energy helium diffraction	[47–51]
	X-ray diffraction	[44,47,48,52,53]
	Infrared spectroscopy	[29,54–59]
	Scanning tunnelling microscopy	[49,60–71]
Composition	X-ray photoelectron spectroscopy	[25,33,55,56,72]
Wettability	Contact angle	[13,31,33,73–77]
Thickness of the adsorbed layer(s)	Ellipsometry	[29,32]
Degree of perfection and electrical properties	Electrochemical methods	[29,43,60,75,78–84]

pits in the gold, 2.4 Å deep, linked by domain boundaries (slightly depressed regions, where the packing is distorted). It is important to note, however, that the holes are still covered with SAMs.

Defect densities are a primary determinant of the suitability of SAMs for use in micro- and nanofabrication. Estimates for the minimum number of defects for SAMs on Au over relatively large areas (several cm^2) range from two to several thousand pinholes per cm^2; the latter value is more realistic [16,85; X.M. Zhao, J.L. Wilbur and G.M. Whitesides, unpublished results]. A stringent test using a wet-chemical etchant to amplify the defects in SAMs gives 90 defects mm^{-2} as a minimum value for the defect density for a SAM of hexadecanethiolate (HDT) on 20 nm thick gold.

With chemical control over the length of the methylene chains, the height of the monolayer perpendicular to the plane of the surface can be controlled with 0.1 nm scale precision. Organic and inorganic synthesis also facilitates the incorporation of different functional groups into, and at the termini of, the alkyl chains: hydrocarbons, fluorocarbons, acids, esters, amides, alcohols, nitriles, and ethers are a few of the many possible functional groups. Mixed monolayers — either with regard to alkyl chain length or chemical functionality — afford further control over surface modification and are prepared by simultaneous coadsorption of two different thiols.

Figure 11.2 shows how interfacial properties such as wetting and adhesion are controlled by SAMs of varying functionality. Water preferentially condenses on regions of a surface patterned with SAMs terminated by hydroxy (OH) groups (patterning techniques are discussed below); the water drops do not form (prior to coalescence) on the regions of the surface covered with SAMs terminated by methyl (CH_3) groups.

SAMs are capable of passivating certains surfaces, and of protecting these surfaces from chemical attack. SAMs of alkanethiols on Cu [86] and GaAs [87,88] have been shown to inhibit oxidation by retarding oxygen transport to the surface. Fe and Ni have

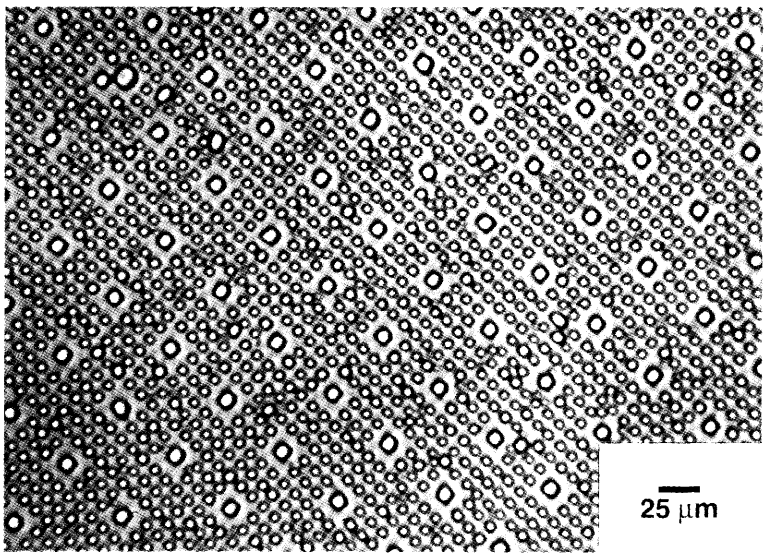

Figure 11.2 Water droplets formed by condensation on regions of a surface (dark) that are covered with a self-assembled monolayer (SAM) that has a hydrophilic head group (e.g. -OH). Water does not condense on other regions of the surface (light) that are covered with an SAM that has a hydrophobic head group (e.g. $-CH_3$).

Table 11.3 Substrates and ligands that form self-assembled monolayers.

Surface	Ligand	Refs
SiO_2, glass	$RSiCl_3$, $RSiOR_3$	[95–100]
Si	$[RCOO]_2$ (neat)	[101]
Si	$RCH=CH_2$, $[RCOO]_2$	[102]
Ag	RSH	[47,48,54,103–105]
GaAs	RSH	[87,106,107]
Cu	RSH	[55,86,108,109]
InP	RSH	[110]
Au	R_3P	[111]
Au	RSO_2H	[112]
Pt	RNC	[113]
Pt	RSH, ArSH	[45,113–116]
Metal oxides	RCOOH	[52,73,117–127]
Metal oxides	RCONHOH	[128]
ZiO_2	RPO_4H_2	[129,130]
In_2O_3/SnO_2 (ITO)	RPO_2H_2	[131]

also been protected from corrosion by other types of thin films [89]. SAMs are also excellent insulators both in, and perpendicular to, the plane of the monolayer: a well-formed C_{18} SAM reduces the current passing across a gold electrode by roughly 10^6 (relative to an underivatized surface), with the residual current attributed to defects. SAMs have also been designed for studies of electrochemistry: ferrocene-terminated monolayers have been used in fundamental studies of the dependence of the rate of electron transport through SAMs on the thickness of the SAM [90]. Many other thiol ligands have been made in order to enhance the electrical properties of SAMs. These include thiol-terminated polythiophene and polyphenylene chains [91,92] and SAMs of polypyrrole-terminated alkanethiols [93,94].

2.2 *Other systems*

Table 11.3 summarizes the wide variety of ligands and substrates that may be used in the formation of self-assembled monolayers.

3 Patterns in two dimensions: microcontact printing (μCP)

3.1 *μCP of alkanethiolates on gold*

Some applications of SAMs in micro- and nanofabrication require that they can be patterned in the plane of the substrate. Techniques to pattern SAMs include microcontact printing (μCP) [85,132,133], micromachining [37,134,135], photolithography/liftoff [136], photochemical patterning [137,138], photo-oxidation [139–142], focused ion beam writing [143], electron-beam writing [87,144–154], STM writing [62,145, 149,155,156], and microwriting with a pen [157,158]. Of these methods, microcontact printing (μCP) is the most versatile, and will be discussed in detail for SAMs of alkanethiolates on gold.

Figure 11.3 shows a schematic of the μCP process. An elastomeric stamp with

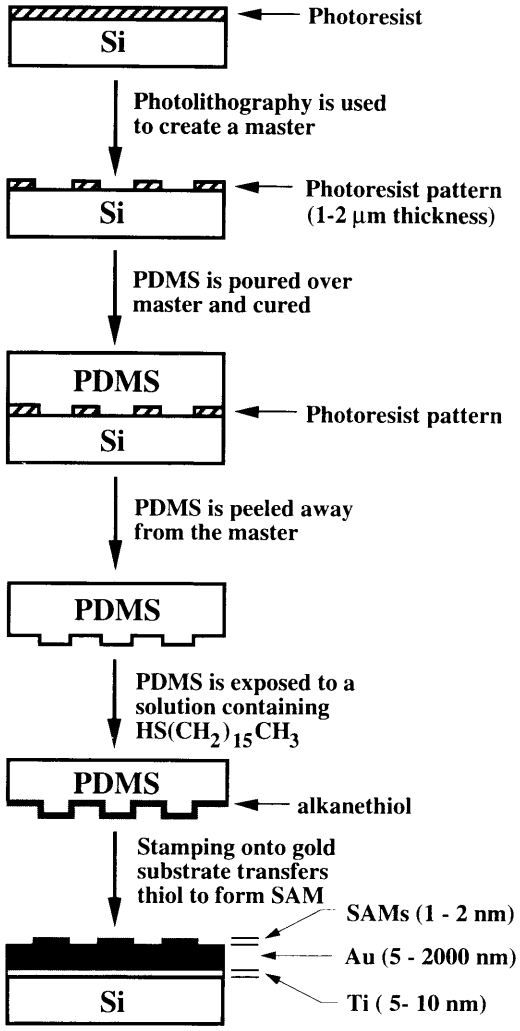

Figure 11.3 Schematic of procedure for microcontact printing.

three-dimensional relief is formed by casting polydimethyl siloxane elastomer (PDMS, Dow-Corning Corporation, Sylgard 184) on a master. Masters are typically prepared by photolithography. Other techniques for the fabrication of masters include electron beam lithography and micromachining; commercial objects with existing relief structure (diffraction gratings, for example) can also be used. Microcontact printing involves several steps.

1 The stamp is inked by applying a dilute (~1 mM) ethanolic solution of alkanethiol to the surface of the stamp with a cotton swab.

2 The stamp is blown dry for 10–20 s with a stream of dry nitrogen.

3 The stamp is placed on a gold-coated substrate (light pressure is sometimes applied to assure conformal contact between the stamp and the gold).

4 SAMs are formed in the regions of contact between the stamp and the surface.

5 The stamp is peeled from the surface.

The underivatized regions of gold can be selectively etched, after μCP, to produce structures of gold. These gold structures can be used subsequently as resists for etching the underlying substrates. Alternatively, SAMs of the same or a different alkanethiolate

can be formed on the underivatized regions by a second μCP step, or by washing the surface with a dilute solution of an alkanethiol.

Several properties of the elastomeric PDMS stamp are critical for the high resolution and the degree of perfection of the patterned SAMs formed by μCP [2,159].

1 In most cases, SAMs are only formed on the surface where there is conformal contact of the stamp with the gold (for appropriate alkanethiols and contact times, see below). PDMS is deformable enough such that contact is achieved even on surfaces with significant roughness [160].

2 The elastomer is sufficiently rigid that the relief structure of the stamp retains its shape.

3 PDMS has a low interfacial free energy (22.1 dynes cm^{-1}) [161] so it does not adhere irreversibly to the surface of the gold.

4 PDMS swells in ethanol; this characteristic allows the stamp to absorb the alkanethiol ink.

The details of the process by which alkanethiol transfers from the stamp to the substrate are not completely understood. Because the stamps are elastomeric in nature, μCP offers some immediate advantages over traditional patterning techniques such as photolithography: patterns can be introduced on curved surfaces [162].

A number of alkanethiols can be used for μCP on gold surfaces. Hexadecanethiol (HDT) is particularly well suited for μCP because it is autophobic and has low volatility. Non-autophobic alkanethiols [163–166] such as $HS(CH_3)_{15}COOH$ can spread reactively after application to the gold in air and do not yield high resolution patterns smaller than 1–2 μm. To reduce reactive spreading, non-autophobic alkanethiols have been stamped under water [167]. Alkanethiols shorter than HDT can be too volatile for use in μCP: SAMs can form from alkanethiol vapour in regions not in contact with the stamp.

Figure 11.4(a) shows a scanning electron microscopy (SEM) image of a master that was prepared by photolithography. Figure 11.4(b) shows an SEM image of patterned SAMs formed with μCP using an elastomeric stamp that was cast from the master shown in Fig. 11.4(a). These images represent the level of complexity, perfection, and scale of features that can be produced routinely by μCP. Figure 11.4(c) shows a lateral force micrograph [160] of a test pattern of SAMs terminated by two different alkanethiols. SAMs terminated by CH_3 (dark stars in the image) were formed by μCP with HDT; SAMs terminated by COOH were deposited (in regions of the gold not derivatized by μCP) by washing the substrate with a dilute, ethanolic solution of $HS(CH_3)_{15}COOH$. The edge resolution between regions terminated by CH_3 and COOH was 50 nm [160]. The smallest pattern generated to date with μCP is 200 nm lines separated by 200 nm spaces [168].

Microcontact printing is an attractive technique because it is simple, inexpensive, and flexible. The cost of PDMS elastomer is negligible, many stamps can be cast from one master, and each stamp can be used hundreds of times. The process is inherently parallel in that large areas (many cm^2) can be patterned at once. Routine access to a clean room is not required, although occasional use of a clean room is convenient to make the photolithographic masters. Areas of future research in the development of μCP include the generation of smaller scale patterns (< 100 nm), minimization of the number of defects in the patterns, and the registration and alignment of patterns over large areas or in multiple printing steps.

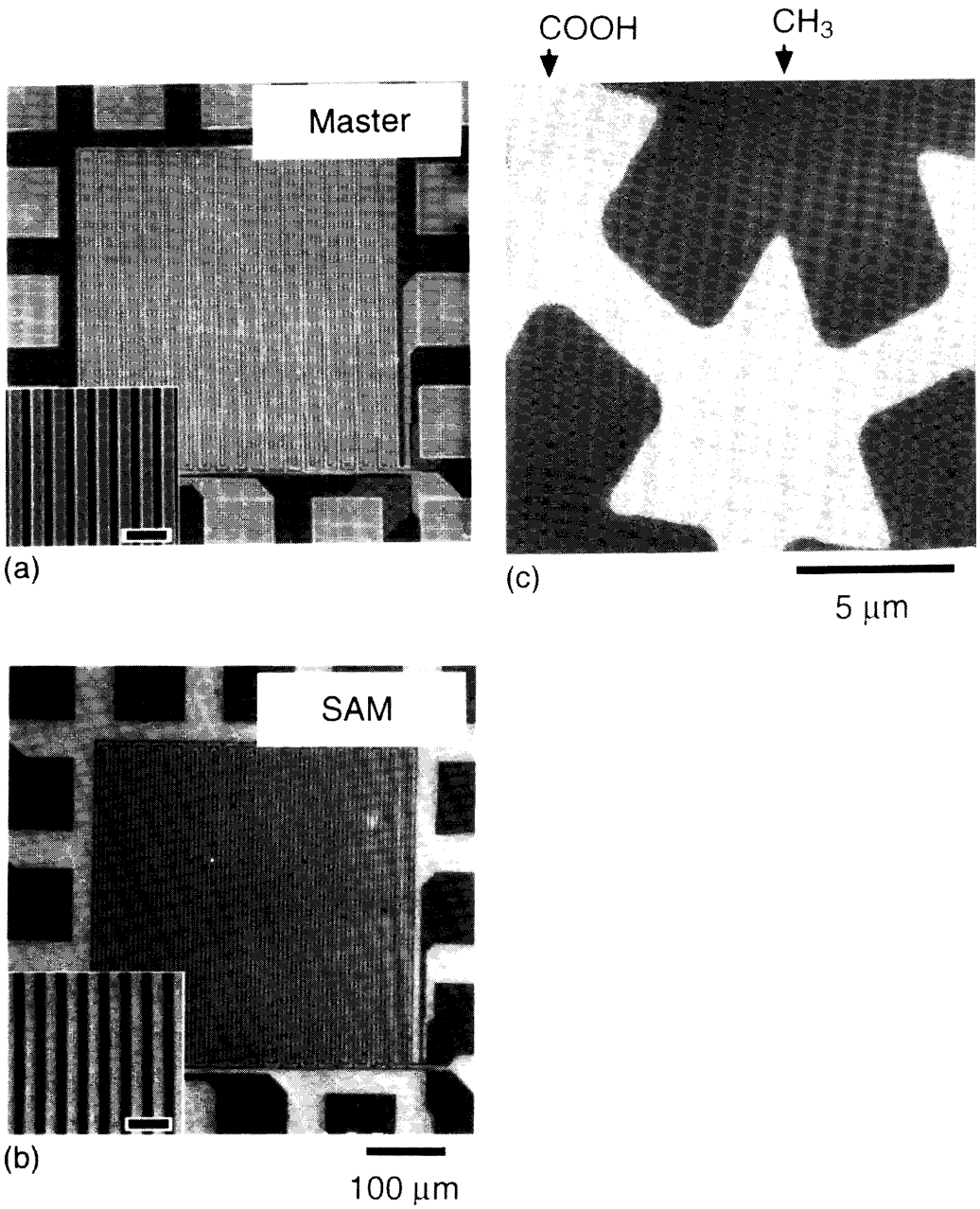

Figure 11.4 (a) Scanning electron micrograph (SEM) of a master with three-dimensional relief that was used to cast stamps for microcontact printing (μCP). The contrast in the image results from height differences between regions, and also from different materials on the surface in the relief structure. (b) SEM image of a patterned self-assembled monolayer (SAM) formed by microcontact printing. The dark regions of the surface are covered with SAMs, and the light regions are underivatized gold. The scale bars in the inserts correspond to 10 μm. (c) Lateral force micrograph of a patterned SAM. Relatively high frictional forces between the probe tip and the surface are detected in regions (light) covered with a carboxy-terminated SAM, and relatively low frictional forces are detected over regions (dark) covered with a methyl-terminated SAM.

Feature sizes of approximately 100 nm in patterned SAMs have been fabricated by adapting the μCP process. In one procedure, mechanical compression of the stamp produced features ca five times smaller than those originally cast from the master [169]. In another process, stamps with small feature sizes were cast from masters prepared by anisotropic etching of silicon [168]. Alternatively, controlled reactive spreading of 4 non-autophobic alkanethiols also produced features of dimension 100 nm [170].

3.2 *μCP of other materials*

Microcontact printing (μCP) has been used in systems other than alkanethiols on gold. Patterned SAMs have been formed with alkanethiols on copper [171], alkanethiols on silver [172], and with alkyltrichlorosilanes on Si/SiO_2 and glass [173]. The latter system is particularly useful because: (i) coinage metals (which are often incompatible materials for silicon microelectronic devices) are not necessary; (ii) SAMs formed from alkyltrichlorosilanes have higher thermal stability than SAMs of alkanethiolates on gold; (iii) patterned SAMs on glass are desirable for optical applications. SAMs formed from alkyltrichlorosilanes take longer to form and are not as highly ordered as SAMs of alkanethiolates on gold; they are also not as effective as chemical resists [173]. The edge resolution in μCP of alkyltrichlorosilanes on Si/SiO_2 or glass is currently ~200 nm [174] compared with the edge resolution of 20–50 nm [175] observed in the alkanethiolate/gold system.

Microcontact printing of liquids containing suspended palladium colloids [175] has also been demonstrated. Features with dimensions on the micron- and submicron-scale were prepared with edge resolution of approximately 100 nm. Colloids can be deposited on a variety of substrates including glass, Si/SiO_2, and polymers. Following deposition, the palladium can act as a catalyst for electroless deposition of metals. These experiments indicate that μCP may be a general technique that can be used in systems other than SAMs.

4 Fabrication of three-dimensional structures

4.1 *SAMs as ultrathin resists*

Problems in optical lithography concerning depth of focus, optical transparency, shadowing and undercutting for the fabrication of features of sub-50-nm dimensions result from the inability to produce sufficiently thin films of photoresist (<20 nm). The use of SAMs as resists potentially resolves these problems because the thickness of the monolayer is ~1–2 nm. SAMs are capable of protecting the underlying substrate from corrosion by wet-chemical etchants [176]. Relative capabilities are determined by the length of the alkyl chain and the nature of the terminal functional group [134].

Figure 11.5 shows a series of metal structures that were fabricated using patterned SAMs of HDT formed by μCP as resists. The underivatized regions were etched by a solution of ferricyanide, or with a basic, oxygenated cyanide etch [3,172,176]. The derivatized sections were barely affected by the etch in the time required to remove the underivatized gold (Figs 11.5a–c) or silver (Fig. 11.5d). Silver etches more quickly and

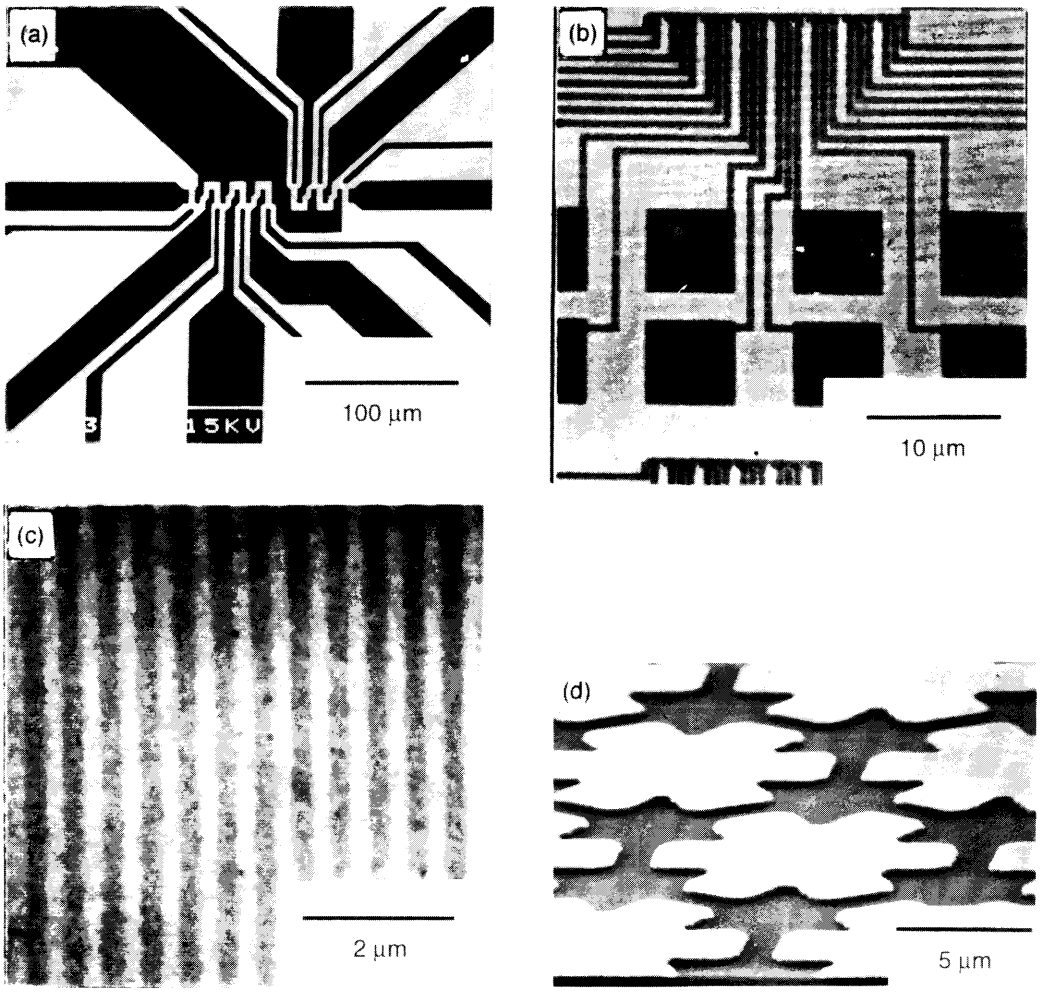

Figure 11.5 Metal structures [(a, b, c) gold, (d) silver] fabricated using patterned self-assembled monolayers [SAMs; formed by microcontact printing (μCP)] as resists. The underivatized metal is etched with a solution of ferric cyanide (a, d) or with a basic oxygenated cyanide solution (b, c). The 200 nm lines of gold separated by 200 nm wides spaces of Si/SiO_2 are the smallest structures fabricated to date by μCP.

with better resolution than gold [172]. This technique is capable of producing 200 nm features (Fig. 11.5c) [168] with edge resolution of ~20 nm.

Microcontact printing of patterned SAMs and selective etching was used to fabricate gold features on non-planar surfaces [162]; the capability to work on non-planar substrates is beyond the capabilities of routine photolithography. Figure 11.6 shows clearly resolved features of gold with dimensions of a few microns on curved surfaces with diameter 500 μm (Fig. 11.6a–b) and diameter 50 μm (Fig. 11.6c).

The gold (or silver) features can act as secondary resists for further substrate etching [85,168,174,177,178]. Complex silicon structures were fabricated with features as small as 100 nm. A typical fabrication process involves the following steps; (i) titanium (1.5–5 nm) and then gold (15–100 nm) are evaporated onto a Si [99] wafer; [ii] a patterned SAM is formed by μCP; (iii) underivatized regions of gold are etched with a basic ferricyanide solution to create a gold structure based on the pattern of the SAM;

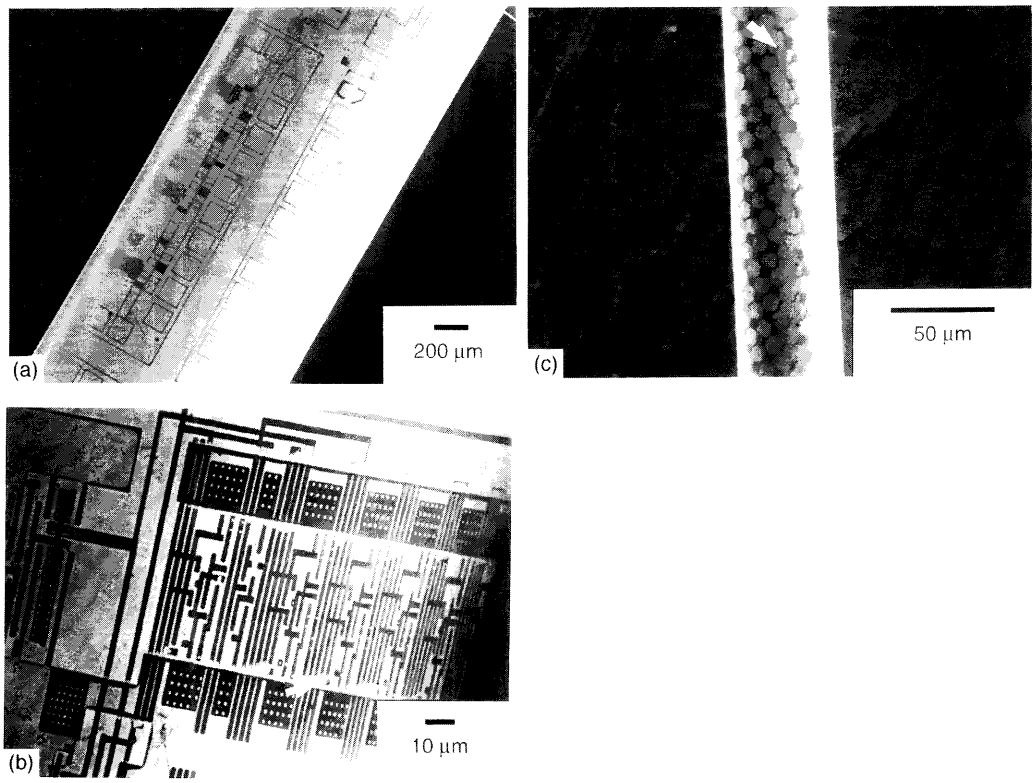

Figure 11.6 (a, b) Scanning electron micrograph (SEM) image of gold microstructures formed by microcontact printing (μCP) with HDT on a gold-coated capillary (r = 500 mm), followed by etching. A number of defects are apparent in (b) (white arrow); these defects originated in the master used to cast the stamp. (c) SEM image of patterned gold structures formed on a 50 mm diameter gold-coated glass fibre. There was a stripe (white arrow) where the capillary was printed twice when it rolled more than 360°. Light regions in these images correspond to gold; dark regions are Ti/TiO_2/glass where etching removed the gold. [Reprinted with permission from Jackman RJ, Wilbur JL, Whitesides GM. *Science* 1995; **269**: 664. Copyright (1995) American Association for the Advancement of Science].

(iv) the titanium layer and native SiO_2 layer are removed by dissolution in 1% HF; (v) the silicon wafer is etched anisotropically (15% solution by volume of 4 M KOH in *i*-PrOH, at 60°C for time periods proportional to the desired etch depth) using the gold pattern as a resist; and (vi) the remaining gold and titanium are removed by exposure to aqua regia (1 : 1 HNO_3 : HCl). Figure 11.7(a) shows a gold grid fabricated by μCP and subsequent etching of regions not covered with SAMs. Figure 11.7(b) shows the resulting pyramid-shaped 'pits' in the substrate after anisotropic etching of silicon. Figures 11.7(c)–(d) are SEM images of more complex silicon structures that were formed with this same process.

Microlithography using neutral metastable argon atoms [179] has been investigated as a technique for patterning and fabricating surface features with high resolution (<100 nm); beams of the neutral atoms have de Broglie wavelengths of order 0.01 nm, and can in principle be focused to a spot that is limited by the size of the atom. Conventional resists cannot be patterned with these beams because damage from the metastable argon atoms is restricted to a surface layer less than 0.5 nm thick. This depth, however, is sufficient to damage SAMs of HDT on gold such that an aqueous

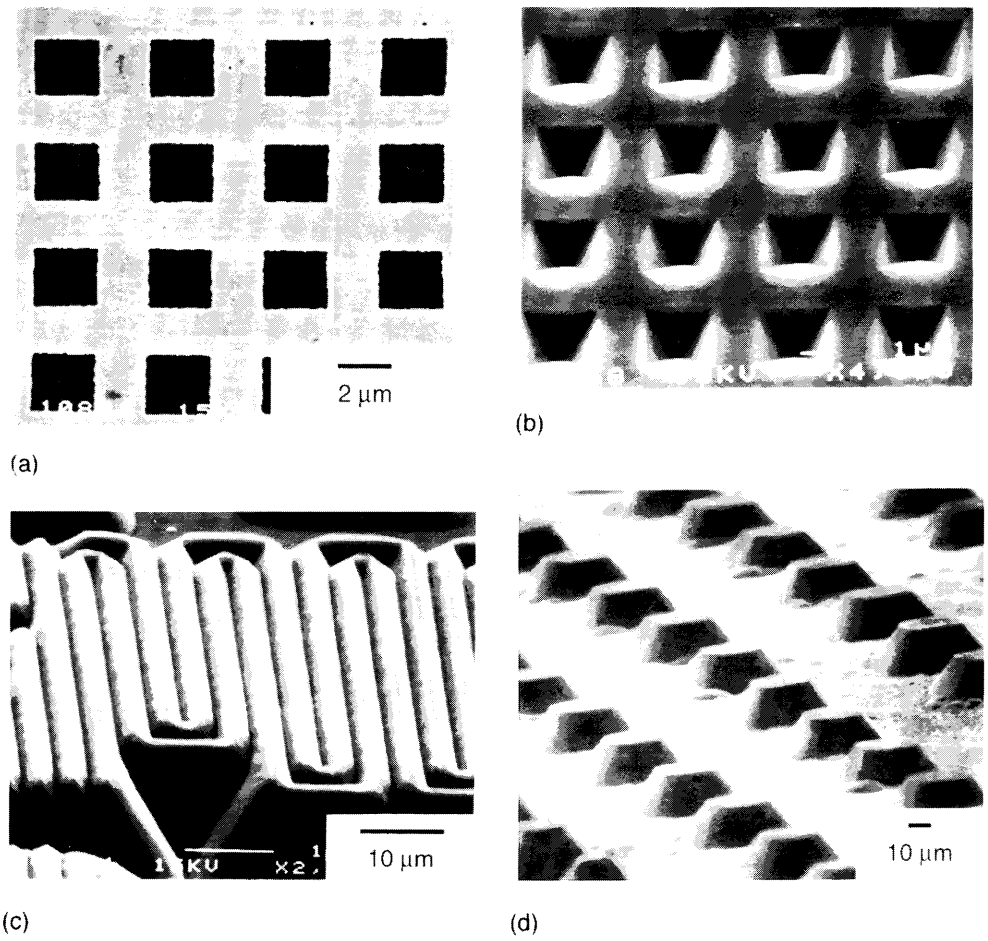

Figure 11.7 (a) Scanning electron micrograph (SEM) of a grid of gold fabricated by microcontact printing (μCP) and selective etching of gold. The dark regions are the underlying silicon. (b) Selective anisotropic etching of the silicon in (a) results in 'pits' that are inverted pyramids. (c–d) SEMs of etched silicon structures using gold patterns (formed by μCP and etching) as resists.

ferricyanide solution will etch the metal under the exposed regions. Figure 11.8 shows a schematic of the process, an SEM image of a copper TEM grid used as a mask (in contact with the surface of the substrate), and an SEM image of the gold structure that was fabricated using the TEM grid as a mask.

4.2 *Templated adsorption*

SAMs are essentially two-dimensional structures. The techniques for fabrication described above focused on the use of SAMs as resists; the pattern in the SAMs was transferred to the underlying substrate by selective etching to produce a structure with three-dimensional features. Materials can also be assembled on the surface of patterned SAMs to build three-dimensional structures.

Patterned SAMs that consist of regions of bare gold and regions covered by SAM have been used as templates for assembling polymeric structures [180] and metal structures [150,151] with electrochemistry, and metal structures with chemical vapour

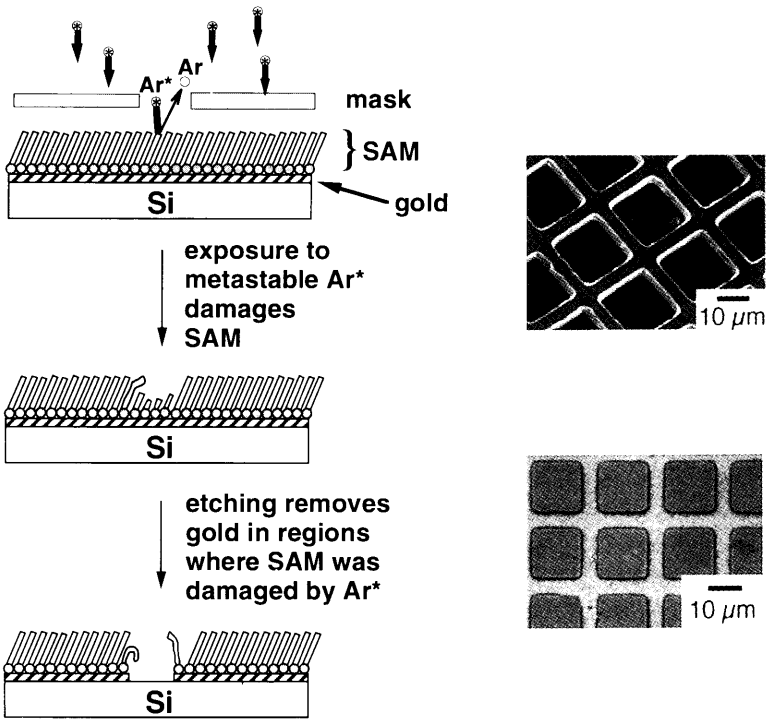

Figure 11.8 The scheme represents exposure of self-assembled monolayers of dodecanethiol (~1.5 nm thick) on gold (20 nm with 1.5 nm of titanium) to a beam of metastable Ar, followed by wet-chemical etching. The SEM pictures are of the copper TEM grid (~10 nm thick) used as a mask (in contact with the surface of the substrate), and the resulting fabricated gold structure.

deposition [156,181–183] and electroless deposition [85]. The insulating properties of SAMs inhibit deposition in these processes in selected regions. Figure 11.9(a) shows a schematic of a procedure to pattern a silicon structure with SAMs of $CH_3(CH_2)_{17}SiCl_3$ by μCP with a flat stamp on a surface with relief. Copper is deposited on regions not covered with SAMs by chemical vapour deposition (Fig. 11.9b) [183].

Other assembly processes take advantage of our ability to pattern SAMs with different organic functional groups. Different regions of the substrate can be tailored to have different surface free energies and different wettabilities. For example, a surface patterned with SAMs terminated by a methyl group and SAMs terminated by a carboxy group has regions that are extremely hydrophobic (CH_3) and hydrophilic (COOH), respectively. When such a surface is exposed to water vapour at low temperatures or at high humidity, water droplets preferentially condense on the hydrophilic regions (see Fig. 11.2). These droplets or 'condensation figures' have been used to image patterned SAMs [158], as sensors for monitoring humidity and temperature [85], and as optical diffraction gratings [184].

Figure 11.10 shows a schematic of a process to fabricate solid three-dimensional structures based on the different wetting properties of patterned SAMs. Hydrophilic regions are formed on a gold surface by microcontact printing with $HS(CH_2)_{15}COOH$. All other regions of the gold surface are made hydrophobic by immersing the sample into a dilute solution of HDT in ethanol. The sample is then slowly pulled from a prepolymer liquid (for example, UV-curable polyurethanes, Norland Optical Adhesives 60, 61 or 81) through an interface into air. The prepolymer liquid preferentially wets

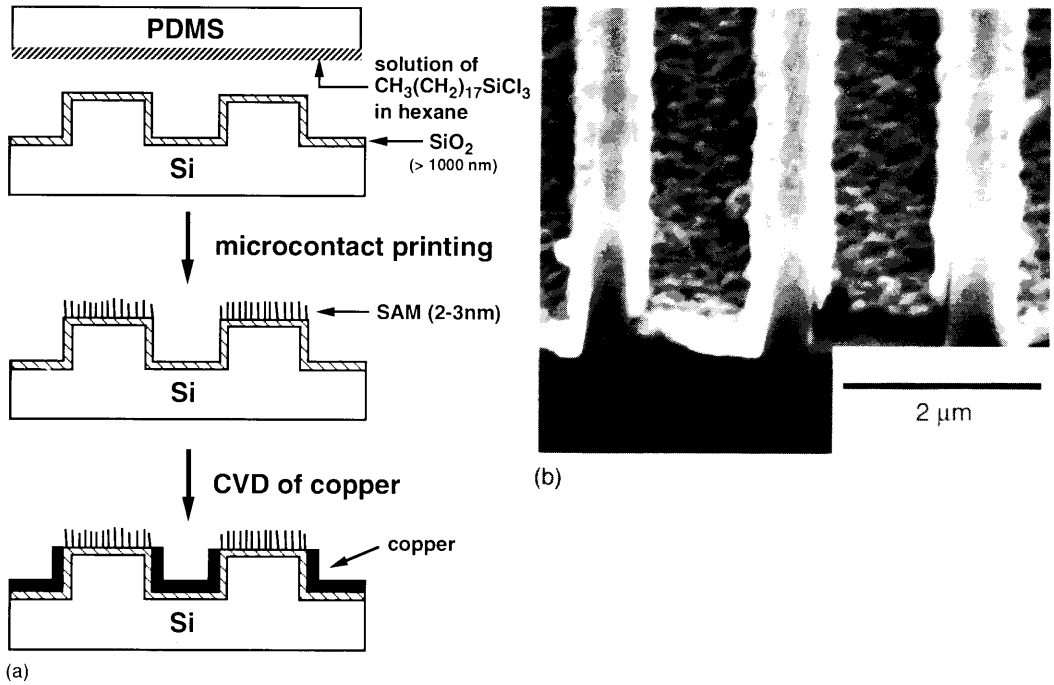

Figure 11.9 (a) Schematic outline of the procedure used for patterning alkylsiloxanes on a non-planar substrate. Nucleation and deposition of copper only occurs on those regions underivatized by the self-assembled monolayer in the following process of selective CVD. (b) Scanning electron micrograph of a microstructure of copper fabricated by CVD on a substrate whose surface was derivatized by a monolayer of octadecyltrichlorosilane. The specimen has been fractured in cross-section to reveal the copper morphology and coverage — here ~200 nm. Copper deposits only in recessed regions not covered by alkylsiloxane (the tops of the ridges).

the hydrophilic regions of the surface, assumes a shape to minimize its free energy, and does not adhere to the hydrophobic regions. The structure is solidified by curing the polymer in place by exposure to UV light. The smallest structures we have fabricated in this way have lateral dimensions of ~3 μm, and rise above the plane of the sample by a few microns. Optical waveguides with lengths as long as 2–3 cm have been fabricated using a similar process [185]. Figure 11.11(a) and (b) shows these waveguides in cross-section, and Fig. 11.11(c) shows the multimode output from a waveguide.

Hydrocarbon liquids can also be assembled on hydrophobic regions of patterned SAMs by pulling the substrate from the liquid through an interface into water [159,186] (instead of air). Again, the process of assembly is controlled by the minimization of free energies. In the case of assembling the polyurethane prepolymers on patterned SAMs, the final structures rise higher above the surface when fabricated on hydrophobic regions in water than when fabricated on hydrophilic regions in air because the surface tension of water is greater than the surface tension of air. Figure 11.11(d) shows an atomic force micrograph of an array of polymeric lenses [159] that were assembled on hydrophobic regions of a patterned SAM in water. The pattern in this case was circles (~10 μm diameter) of SAMs of HDT in a background of SAMs of $HS(CH_2)_{15}OH$.

As discussed earlier, palladium colloids can be patterned by μCP on a variety of surfaces [175]. Figure 11.12 shows a schematic of the procedure for patterning the colloids, and an SEM image depicting the scale and perfection of the copper structures

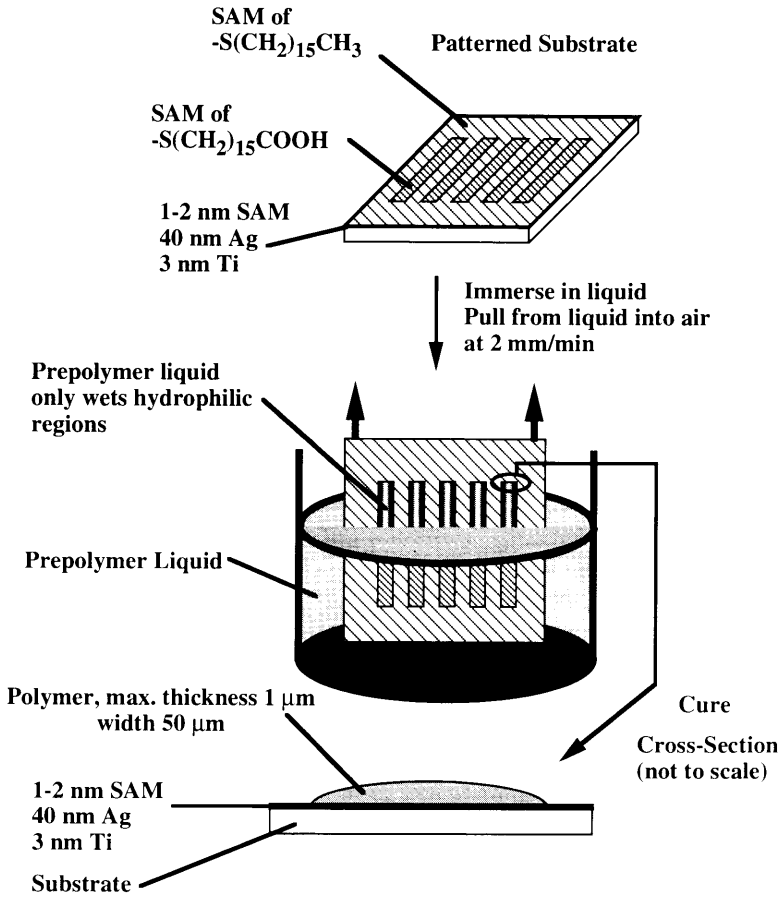

Figure 11.10 Schematic of the process of assembling liquids on patterned self-assembled monolayers (SAMs). The liquid preferentially wets the hydrophylic regions (carboxy-terminated SAM) of the surface, and de-wets from the hydrophobic regions (methyl-terminated SAM) of the surface. Liquid prepolymers are cured after assembly to fabricate solid three-dimensional structures.

that can be fabricated by using the colloids as templates for electroless deposition of copper.

4.3 *Micromoulding in capillaries (MIMIC)*

Patterning techniques are well established for semiconductors and metals, but are relatively underdeveloped for organic polymers, with the notable exception of the specialized polymers used in photolithography. Methods to pattern polymers based on the preferential wetting of patterned SAMs by liquid polymer precursors were discussed above. Micromoulding in capillaries (MIMIC) [187] is another technique to pattern polymers that uses many of the materials described above, but achieves patterning by completely different principles. Figure 11.13 shows a schematic of the MIMIC process. An elastomeric stamp is placed in conformal contact with a substrate to form a mould that consists of a network of channels. A low viscosity polymer precursor is placed in contact with openings to the network, and the channels fill by capillary action. After curing the polymer precursor, the elastomeric stamp is removed. The patterned

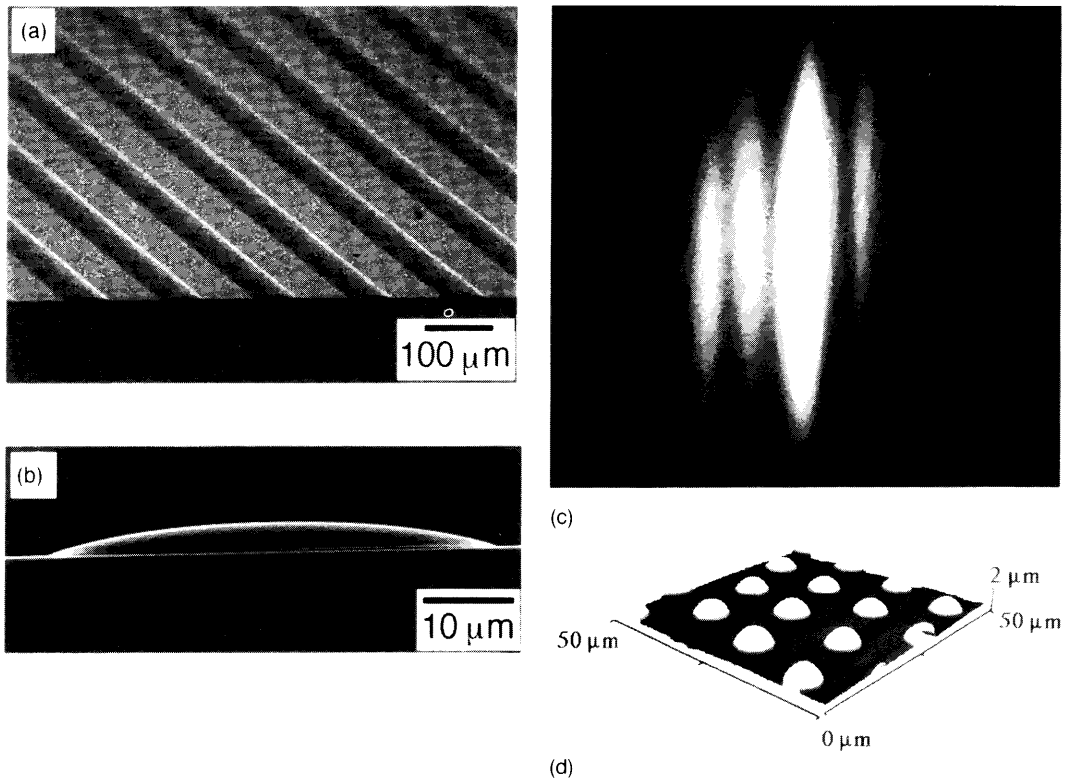

Figure 11.11 (a, b) Scanning electron micrograph (SEM) images of polymeric waveguides that were fabricated by assembling prepolymer liquids (Norland Optical Adhesive 60, polyurethane) on patterned self-assembled monolayers (SAMs) (as in Fig. 11.9). (c) Projection of the laser output from a waveguide 1 cm in length. (d) AFM image (constant force mode) of an array of polyurethane lenses that were assembled on a patterned SAM.

polymer does not adhere to the stamp, and remains on the support. Under certain conditions, the patterned polymer was subsequently detached from the substrate to produce a free standing film. Figure 11.14 shows examples of polymeric structures that were fabricated using MIMIC.

As a method to produce polymeric microstructures, MIMIC [187] holds several advantages over conventional photolithography. Photolithography requires the use of specialized polymers and photosensitizers; MIMIC is applicable to most polymers with low viscosity. Photolithography requires three steps: (i) spin coating to form a film; (ii) patterning (by exposure to light); and (iii) developing exposed (or unexposed) regions to fabricate microstructures. MIMIC forms and patterns polymeric microstructures in a single step. In photolithography, the polymeric microstructure formed in each exposure must be the same thickness; with MIMIC, patterning structures with multiple thicknesses is possible. Like the masks employed in conventional photolithography, the stamps used as templates for MIMIC can be reused.

4.4 *Micromachining of electrodes*

Gold electrodes were fabricated using a combination of micromachining and SAMs [134]. In one procedure, SAMs of HDT were formed over the entire surface of a

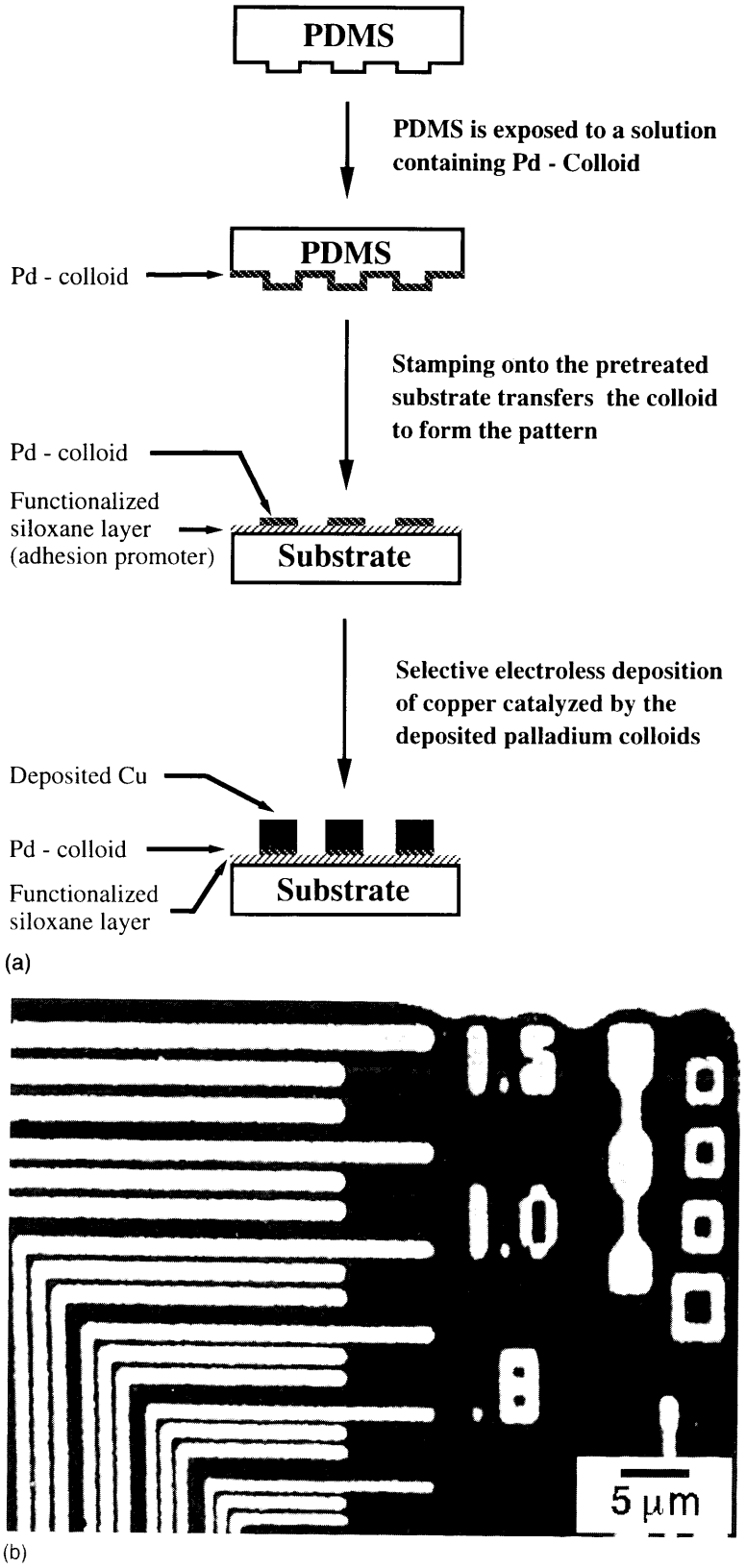

Figure 11.12 (a) Schematic illustration of the process to pattern surfaces with Pd colloids with microcontact printing. The Pd colloids are used to catalyse the electroless deposition of Cu on specific regions of the substrate. (b) Scanning electron micrograph (SEM) image of Cu structures that were fabricated with the process described above.

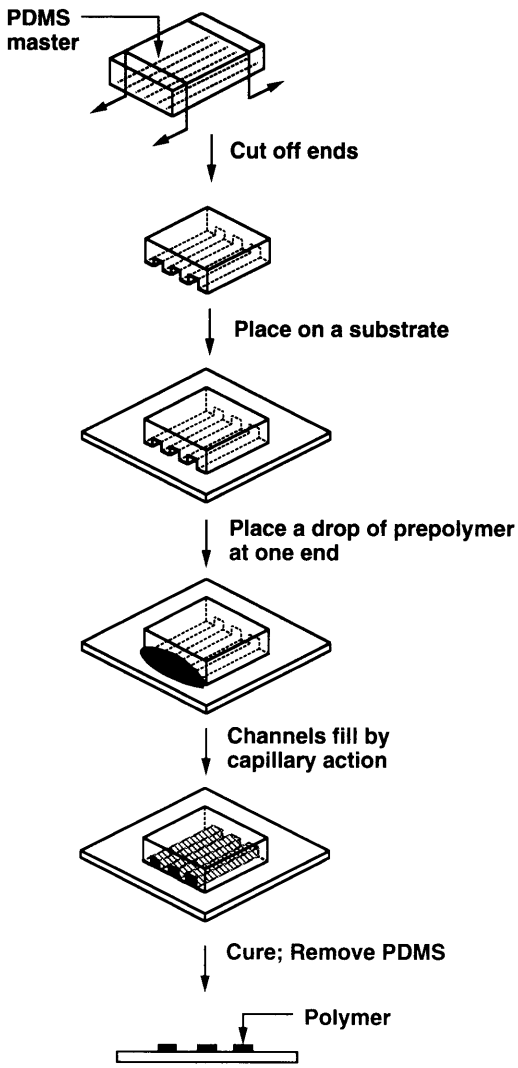

Figure 11.13 Schematic diagram of capillary micromoulding of a pattern of parallel, rectangular channels. It is not necessary for both ends of the channels to be open: even if one end is closed, the channels fill with the prepolymer. The trapped air seems to escape by diffusing through the polydimethyl siloxane (PDMS) master.

gold-coated substrate, and bare gold was exposed in patterns of lines on the substrate by scratching the surface using the tip of a surgical scalpel blade. Large area (>0.1 mm^2) arrays of band type electrodes (1 μm wide) were fabricated in this way; the exposed gold forms the electrochemically active surface of the electrode. In a second procedure, SAMs of $HS(CH_2)_2OH$ were deposited on the gold surface, lines were micromachined, and the exposed gold was derivatized with HDT. The regions of gold covered with $HS(CH_2)_2OH$ were subsequently etched with an aqueous solution of CN^- saturated with O_2, and the gold wires that remained were micrometre wide, centimetre long, and 100 nm thick. Paired electrodes with electrochemically active areas as small as 100 nm × 1 μm were fabricated from these structures by machining a 1 μm gap into the supported gold wire (still covered with an electrically insulating SAM of HDT). The exposed gold on either side of the gap is electrochemically active.

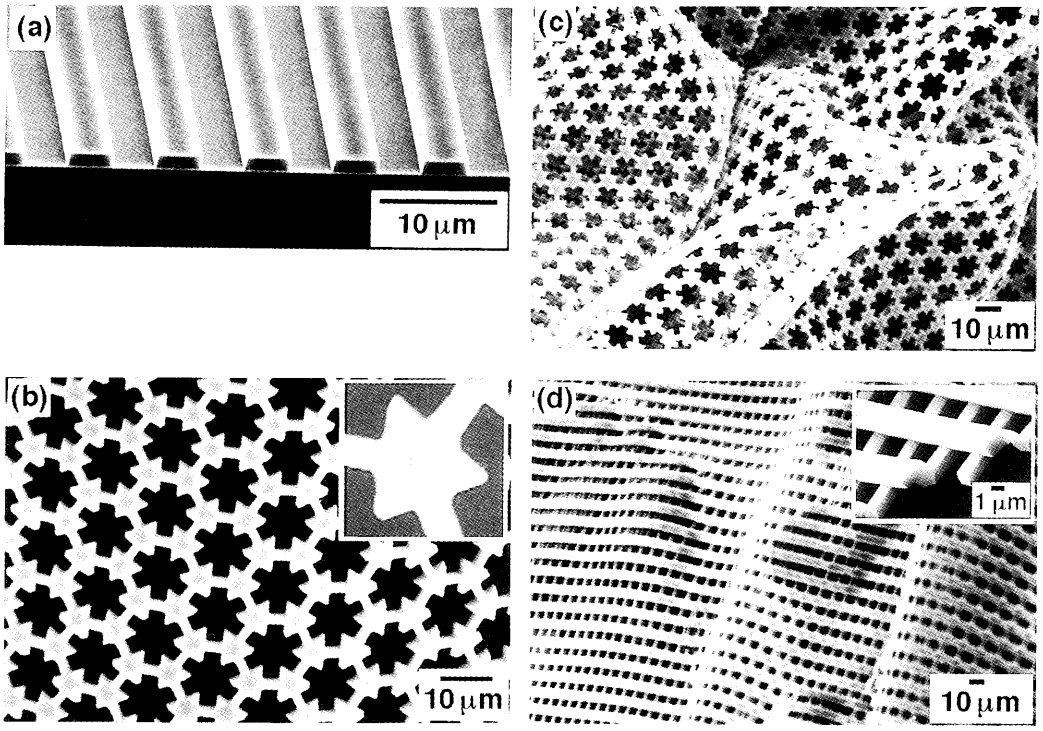

Figure 11.14 Patterns fabricated by micromoulding in capillaries (MIMIC). Patterns were sputtered with gold before imaging by scanning electron microscopy. The polymer used was photocured poly(methylmethacrylate). (a) An oblique image of a fractured sample showing rectangular slabs of polymer on a gold film supported on Si/SiO_2. (b) Image (captured at 30°) of more complex patterns on a silicon wafer. (c) A free-standing film: the same film as in (b) was released from the surface by dissolving the SiO_2 layer in NH_4F/HF. The folding in this region of the sample was accidental, but illustrates the flexibility of the film. (d) A free-standing polymeric structure fabricated in channels formed by conformal contact of two polydimethyl siloxane (PDMS) masters like those in (a), using an orientation in which the grooves of the two masters were perpendicular. The two layers of the channels formed one interconnected polymeric structure (inset). [Reprinted with permission from Kim E, Xia Y, Whitesides GM. *Nature* 1995; **376**: 581. Copyright (1995) Macmillan Magazines Limited.]

5 Conclusions and future directions

Molecular self-assembly is a useful strategy for micro- and nanofabrication, and potentially for other applications in molecular electronics. Equilibrium structures are formed that are at, or close to, thermodynamic minimum [6,7]. These structures tend to be self-healing and defect rejecting [5], and the size of the structures can be in the range of 1–100 nm, a range difficult to address with current fabrication techniques. In particular, systems that by definition have at least one dimension of molecular scale — self-assembled monolayers — have demonstrated applications in microelectronics and micro- and nanofabrication that include passivation of surfaces, use of SAMs for ultrathin resists and masks, directed deposition of materials on surfaces patterned with SAMs, and the use of surface functionality for sensors.

Several issues remain to be resolved, however, before SAMs find real applications in microelectronics. Alkanethiolates on gold are the most developed system of SAMs; the potential applications and techniques for fabrication that we described are based on

this system. Unfortunately, gold is incompatible with silicon processing [27], and SAMs of alkanethiolates on gold are not sufficiently thermally stable for many applications. New systems of SAMs need to be developed that are more compatible with current processes and materials for the fabrication of microelectronic devices. At present, the density of defects in metal structures formed by chemical etching using patterned SAMs as resists is too high for applications in microelectronics, although it is acceptable for many optical systems. The formation and distribution of these defects must be understood to reduce their numbers. To take full advantage of SAMs as ultrathin resists or to use SAMs to fabricate quantum devices (lateral dimensions less than 50 nm [188]), techniques to pattern SAMs at sub-50-nm scales (in the plane of the monolayer) must be developed. SAMs are patterned routinely by microcontact printing [85,132,176] with features of micron dimensions, and these structures form the basis of fabrication techniques that are immediately suitable for applications in optics [159,185] and biotechnology [189–191], if not in microelectronics.

Acknowledgements. We thank Dr Emmanuel Delamarche and Dr Hans Biebuyck for providing the images in Fig. 11.1. The research was supported in part by the Office of Naval Research, ARPA and NSF (PHY 9312572). This work made use of MRSEC Shared Facilities supported by the National Science Foundation (DMR-9400396). J.L.W. gratefully acknowledges a postdoctoral fellowship from the NIH.

6 References

1 Moreau WM. *Semiconductor Lithography: Principles and Materials.* New York: Plenum Press, 1988.
2 Wilbur JL, Whitesides GM. In: Timp G, ed. *Nanotechnology.* Washington, DC: AIP, in press.
3 Xia Y, Zhao XM, Whitesides GM. *Microelectronic Engineering*, in press.
4 Whitesides GM, Mathias JP, Seto CT. *Science* 1991; **254**: 1312.
5 Lindsey JS. *New J Chem* 1991; **15**: 153.
6 McGrath KP, Kaplan DL. *Mater Res Soc Symp Proc* 1994; **330**: 61.
7 Kim E, Whitesides GM. *J Am Chem Soc*, submitted.
8 Varner JE, ed. New York: Alan R. Liss, 1988.
9 Kossovsky N, Millett D, Sponsler E, Hnatyszyn HJ. *Bio/Technology* 1993; **11**: 1534.
10 Creighton TE. *Proteins: Structure and Molecular Properties.* New York: Freeman, 1983.
11 Sanger W. *Principles of Nucleic Acid Structure.* New York: Springer-Verlag, 1986.
12 Bain CD, Whitesides GM. *Angew Chem Int Ed Engl* 1989; **28**: 506.
13 Whitesides GM, Laibinis PE. *Langmuir* 1990; **6**: 87.
14 Ulman A. *J Mater Educ* 1989; **11**: 205.
15 Ulman A. *An Introduction to Ultrathin Organic Films.* San Diego, CA: Academic Press, 1991.
16 Dubois LH, Nuzzo RG. *Annu Rev Phys Chem* 1992; **43**: 437.
17 Bard AJ, Abruna HD, Chidsey CED *et al. J Phys Chem* 1993; **97**: 7147.
18 Whitesides GM, Gorman CB. In: Hubbard AT, ed. *Handbook of Surface Imaging and Visualization.* Boca Raton: CRC Press, in press.
19 de Gennes P-G. *The Physics of Liquid Crystals*, 2nd edn. *International Series of Monographs on Physics*, Vol. 83. New York: Oxford University Press, 1993.
20 Simanek EE, Mathias JP, Seto CT *et al. Acc Chem Res* 1995; **28**: 37.
21 Archibald DD, Mann S. *Nature* 1993; **364**: 430.

22 Heywood B, Mann S. *Chem Mater* 1994; **6**: 311.
23 Noshay A, McGrath JE. *Block Copolymers: Overview and Critical Survey*. New York: Academic Press, 1977.
24 Bain CD, Evall J, Whitesides GM. *J Am Chem Soc* 1989; **111**: 7155.
25 Bain CD, Whitesides GM. *J Am Chem Soc* 1989; **111**: 7164.
26 Ulman A. *Adv Mater* 1991; **3**: 298.
27 Li J, Seidel TE, Mayer JW. *Mater Res Soc Bulletin* 1994; **XIX**: 15.
28 Li T, Weaver MJ. *J Am Chem Soc* 1984; **106**: 6107.
29 Porter MD, Bright TB, Allara DL, Chidsey CED. *J Am Chem Soc* 1987; **109**: 3559.
30 Bain CD, Whitesides GM. *Science* 1988; **240**: 62.
31 Bain CD, Whitesides GM. *J Am Chem Soc* 1988; **110**: 3665.
32 Bain CD, Troughton EB, Tai Y-T, Evall J, Whitesides GM, Nuzzo R. *J Am Chem Soc* 1989; **111**: 321.
33 Bain CD, Biebuyck HA, Whitesides GM. *Langmuir* 1989; **5**: 723.
34 Nuzzo RG, Allara DL. *J Am Chem Soc* 1983; **105**: 4481.
35 Troughton EB, Bain CD, Whitesides GM, Nuzzo RG, Allara DL, Porter MD. *Langmuir* 1988; **4**: 365.
36 Weisshaar DE, Lamp BD, Porter MD. *J Am Chem Soc* 1992; **114**: 5860.
37 Abbott NL, Folkers JP, Whitesides GM. *Science* 1992; **257**: 1380.
38 Leff DV, Ohara PC, Heath JR, Gelbart WM. *J Phys Chem* 1995; **99**: 7036.
39 Brust M, Walker M, Bethell D, Schiffrin DJ, Whyman R. *J Chem Soc Chem Commun* 1994; 801.
40 Sondag-Huethorst JAM, Schonenberger C, Fokkink LGJ. *J Phys Chem* 1994; **98**: 6826.
41 Goss CA, Charych DH, Majda M. *Anal Chem* 1991; **63**: 85.
42 Wasserman SR, Biebuyck H, Whitesides GM. *J Mater Res* 1989; **4**: 886.
43 Krysinski P, Chamberlin RV, II, Majda M. *Langmuir* 1994; **10**: 4286.
44 Fenter P, Eberthardt A, Eisenberger P. *Science* 1994; **266**: 1216.
45 Pemberton JE, Bryant MA, Joa SL, Garvey SD. *Proc Spie Int Soc Opt Eng* 1992.
46 Strong L, Whitesides GM. *Langmuir* 1988; **4**: 546.
47 Fenter P, Eisenberger P, Li J *et al. Langmuir* 1991; **7**: 2013.
48 Laibinis PE, Lewis NS. *Chemtracts: Inorg Chem* 1992; **4**: 49.
49 Camillone NI, Esienberger P, Leung TYB *et al. J Chem Phys* 1994; **101**: 11031.
50 Camillone NI, Chidsey CED, Liu GY, Scoles G. *J Chem Phys* 1993; **98**: 3503.
51 Chidsey CED, Liu GY, Scoles G, Wang J. *Langmuir* 1990; **6**: 1804.
52 Samant MG, Brown CA, Gordon JGI. *Langmuir* 1993; **9**: 1082.
53 Fenter P, Li J, Eisenberger P, Ramanarayanan TA, Liang KS. *Mater Res Soc Symp Proc* 1992.
54 Walczak MM, Chung C, Stole SM, Widrig CA, Porter MD. *J Am Chem Soc* 1991; **113**: 2370.
55 Laibinis PE, Whitesides GM, Allara DL, Tao YT, Parikh AN, Nuzzo RG. *J Am Chem Soc* 1991; **113**: 7152.
56 Nuzzo RG, Dubois LH, Allara DL. *J Am Chem Soc* 1990; **112**: 558.
57 Evans SD, Urankar E, Ulman A, Ferris N. *J Am Chem Soc* 1991; **113**: 4121.
58 Arndt T, Schupp H, Schrepp W. *Thin Solid Films* 1989.
59 Sun L, Kepley LJ, Crooks RM. *Langmuir* 1992; **8**: 2101.
60 Sun L, Crooks RM. *Langmuir* 1993; **9**: 1951.
61 Creager SE, Hockett LA, Rowe GK. *Langmuir* 1992; **8**: 854.
62 Kim YT, Bard AJ. *Langmuir* 1992; **8**: 1096.
63 Delamarche E, Michel B, Gerber CH *et al. Langmuir* 1994; **10**: 2869.
64 Delamarche E, Michel B, Kang H, Gerber CH. *Langmuir* 1994; **10**: 4103.
65 Schoenenberger C, Sondag HJAM, Jorritsma J, Fokkink LGJ. *Langmuir* 1994; **10**: 611.
66 Stranick SJ, Kamna MM, Krom KR, Parikh AN, Allara DL, Weiss PS. *J Vac Sci Technol, B* 1994; **12**: 20004.

67 Stranick SJ, Parikh AN, Tao YT, Allara DL, Weiss PS. *J Phys Chem* 1994; **98**: 7636.
68 Bucher JP, Santesson L, Kern K. *Langmuir* 1994; **10**: 979.
69 Gregory BW, Dluhy RA, Bottomley LA. *J Phys Chem* 1994; **98**: 1010.
70 Sondag HJAM, Schonenberger C, Fokkink LGJ. *J Phys Chem* 1994; **98**: 6826.
71 Wolf H, Ringsdorf H, Delamarche E *et al. J Phys Chem* 1995; **99**: 7102.
72 Folkers JP, Laibinis PE, Whitesides GM. *Langmuir* 1992; **8**: 1330.
73 Allara DL, Atre SV, Elliger CA, Snyder RG. *J Am Chem Soc* 1991; **113**: 1852.
74 Laibinis PE, Hickman JJ, Wrighton MS, Whitesides GM. *J Am Chem Soc* 1990; **112**: 570.
75 Chidsey CED, Loiacono DN. *Langmuir* 1990; **6**: 682.
76 Tidswell IM, Rabedeau TA, Pershan PS, Folkers JP, Baker MV, Whitesides GM. *Phys Rev B: Condens Matter* 1991; **44**: 10869.
77 Hautman J, Klein ML. *Mater Res Soc Symp Proc* 1992.
78 Kim JH, Cotton TM, Uphaus RA. *J Phys Chem* 1988; **92**: 5575.
79 Chidsey CED, Loiacono DN. *Langmuir* 1990; **6**: 709.
80 Uosaki K, Sato Y, Kita H. *Langmuir* 1991; **7**: 1510.
81 De LHC, Donohue JJ, Buttry DA. *Langmuir* 1991; **7**: 2196.
82 Hickman JJ, Ofer D, Zou C, Wrighton MS, Laibinis PE, Whitesides GM. *J Am Chem Soc* 1991; **113**: 1128.
83 Chidsey CED, Bertozzi CR, Putvinski TM, Mujsce AM, Thorp HH. *Chemtracts: Inorg Chem* 1991; **3**: 27.
84 Sabatani E, Cohen BJ, Bruening M, Rubinstein I. *Langmuir* 1993; **9**: 2974.
85 Kumar A, Biebuyck HA, Whitesides GM. *Langmuir* 1994; **10**: 1498.
86 Laibinis PE, Whitesides GM. *J Am Chem Soc* 1992; **114**: 9022.
87 Tiberio RC, Craighead HG, Lercel M, Lau T, Sheen CW, Allara DL. *Appl Phys Lett* 1993; **62**: 476.
88 Sheen CW, Shi JX, Maartensson J, Parikh AN, Allara DL. *J Am Chem Soc* 1992; **114**: 1514.
89 Stratmann M, Wolpers M, Losch R, Volmer M. *Bull Electrochem Soc* 1992; **8**: 52.
90 Chidsey CDD. *Science* 1991; **251**: 919.
91 Tour JM. *Adv Mat* 1994; **6**: 190.
92 Pearson DL, Schumm JS, Jones LI, Tour JM. *Polym Prep* 1994; **35**: 202.
93 Willicut RJ, McCarley RL. *Langmuir* 1995; **11**: 296.
94 Sayre CN, Collard DM. *Langmuir* 1995; **11**: 302.
95 Wasserman SR, Tao YT, Whitesides GM. *Langmuir* 1989; **5**: 1074.
96 Wasserman SR, Whitesides GM, Tidswell IM, Ocko BM, Pershan PS, Axe JD. *J Am Chem Soc* 1989; **111**: 5852.
97 Sagiv J. *J Am Chem Soc* 1980; **102**: 92.
98 Netzer L, Sagiv J. *J Am Chem Soc* 1983; **105**: 674.
99 Maoz R, Sagiv J. *J Colloid Interface Sci* 1984; **100**: 465.
100 Hoffmann H, Mayer U, Krischanitz A. *Langmuir* 1995; **11**: 1304.
101 Linford MR, Chidsey CED. *J Am Chem Soc* 1993; **115**: 12631.
102 Linford MR, Fenter P, Eisenberger PM, Chidsey CED. *J Am Chem Soc* 1995; **117**: 3145.
103 Laibinis PE, Fox MA, Folkers JP, Whitesides GM. *Langmuir* 1991; **7**: 3167.
104 Chang SC, Chao I, Tao YT. *J Am Chem Soc* 1994; **116**: 6792.
105 Li W, Virtanen JA, Penner RM. *J Phys Chem* 1994; **98**: 11751.
106 Nakagawa OS, Ashok S, Sheen CW, Maertensson J, Allara DL. *Jpn J Appl Phys* 1991; **30**: 3759.
107 Bain CD. *Adv Mater* 1992; **4**: 591.
108 Laibinis PE, Whitesides GM. *J Am Chem Soc* 1992; **114**: 1990.
109 Smith EL. *Report* 1992; 18.
110 Gu Y, Lin Z, Butera RA, Smentkowski VS, Waldeck DH. *Langmuir* 1995; **11**: 1849.
111 Uvdal K, Person I, Liedberg B. *Langmuir* 1995; **11**: 3145.
112 Chadwick JE, Myles DL, Garrell RL. *J Am Chem Soc* 1993; **115**: 10364.
113 Lee TR, Laibinis PE, Folkers JP, Whitesides GM. *Pure Appl Chem* 1991; **63**: 821.

114 Black AJ, Wooster TT, Geiger WE, Paddon-Row MN. *J Am Chem Soc* 1993; **115**: 7924.
115 Shimazu K, Sato Y, Yagi I, Uosaki K. *Bull Chem Soc Jpn* 1994; **67**: 863.
116 Hines MA, Todd JA, Guyot SP. *Langmuir* 1995; **11**: 493.
117 Bigelow WC, Pickett DL, Zisman WA. *J Colloid Interface Sci* 1946; **1**: 513.
118 Timmons CO, Zisman WA. *J Phys Chem* 1965; **69**: 984.
119 Golden WG, Snyder CD, Smith B. *J Phys Chem* 1982; **86**: 4675.
120 Allara DL, Nuzzo RG. *Langmuir* 1985; **1**: 45.
121 Schlotter NE, Porter MD, Bright TB, Allara DL. *Chem Phys Lett* 1986; **132**: 93.
122 Laibinis PE, Hickman JJ, Wrighton MS, Whitesides GM. *Science* 1989; **245**: 845.
123 Chen SH, Frank CW. *Langmuir* 1989; **5**: 978.
124 Chau L-K, Porter MD. *Chem Phys Lett* 1990; **167**: 198.
125 Tao YT, Lee MT, Chang SC. *J Am Chem Soc* 1993; **115**: 9547.
126 Smith E, Porter MD. *J Phys Chem* 1993; **97**: 8032.
127 Ahn SJ, Mirzakhojaev DA, Son DH, Kim K. *Bull Korean Chem Soc* 1994; **15**: 369.
128 Folkers JP, Gorman CB, Laibinis PE, Buchholz S, Whitesides GM. *Langmuir* 1995; **11**: 813.
129 Cao G, Hong H-G, Mallouk TE. *Acc Chem Res* 1992; **25**: 420.
130 Katz HE. *Chem Mater* 1994; **6**: 2227.
131 Gardner TJ, Frisbie CD, Wrighton MS. *J Am Chem Soc* 1995; **117**: 6927.
132 Kumar A, Whitesides GM. *Appl Phys Lett* 1993; **63**: 2002.
133 Wilbur JL, Kumar A, Biebuyck HA, Kim E, Whitesides GM. *Nanotechnology* 1995; in press.
134 Abbott NL, Rolison DR, Whitesides GM. *Langmuir* 1994; **10**: 2672.
135 Lopéz GP, Biebuyck HA, Harter R, Kumar A, Whitesides GM. *J Am Chem Soc* 1993; **115**: 10774.
136 Kleinfeld D, Kahler KH, Hockberger PE. *J Neurosci* 1988; **8**: 4098.
137 Rozsnyai LF, Wrighton MS. *J Am Chem Soc* 1994; **116**: 5993.
138 Wollman EW, Kang D, Frisbie CD, Lorkovic IM, Wrighton MS. *J Am Chem Soc* 1994; **116**: 4395.
139 Calvert JM, Georger JH, Peckerar MC, Pehrsson PE, Schnur JM, Schoen PE. *Thin Solid Films* 1992; **211**: 359.
140 Tarlov MJ, Burgess DR, Gillen G. *J Am Chem Soc* 1993; **115**: 5305.
141 Dressick WJ, Calvert JM. *Jpn J Appl Phys* 1993; **1**: 5829.
142 Huang J, Dahlgren DA, Hemminger JC. *Langmuir* 1994; **10**: 626.
143 Gillen G, Wight S, Bennett J, Tarlov MJ. *Appl Phys Lett* 1994; **65**: 534.
144 Sondag-Huethorst JAM, van Helleputte HRJ, Fokkink LGJ. *Appl Phys Lett* 1994; **64**: 285.
145 Lercel MJ, Redinbo GF, Craighead HG, Sheen CW, Allara DL. *Appl Phys Lett* 1994; **65**: 974.
146 Marrian CRK, Perkins FK, Brandow SL, Koloski TS, Dobisz EA, Calvert JM. *Appl Phys Lett* 1994; **64**: 390.
147 Rieke PC, Tarasevich BJ, Wood LL *et al.* *Langmuir* 1994; **10**: 619.
148 Mino N, Ozaki S, Ogawa K, Hatada M. *Thin Solid Films* 1994; **243**: 374.
149 Perkins FK, Dobisz EA, Brandow SL *et al.* *J Vac Sci Technol B* 1994; **12**: 3725.
150 Lercel MJ, Redinbo GF, Pardo FD *et al.* *J Vac Sci Technol B* 1994; **12**: 3663.
151 Sondag-Huethorst JAM, van Helleputte HRJ, Fokkink LGJ. *Appl Phys Lett* 1994; **64**: 285.
152 Lercel MJ, Redinbo GF, Rooks M *et al.* *Microelectr Eng* 1995; **27**: 43.
153 Rieke PC, Baer DR, Fryxell GE, Engelhard MH, Porter MS. *J Vac Sci Technol A* 1993; **11**: 2292.
154 Baer DR, Engelhard MH, Schulte DW, Guenther DE, Wang L-Q, Rieke PC. *J Vac Sci Technol A* 1994; **12**: 2478.
155 Ross CB, Sun Li, Crooks RM. *Langmuir* 1993; **9**: 632.
156 Schoer JK, Ross CB, Crooks RM, Corbitt TS, Hampden SMJ. *Langmuir* 1994; **10**: 615.
157 Lopéz GP, Biebuyck HA, Whitesides GM. *Langmuir* 1993; **9**: 1513.
158 Lopéz GP, Biebuyck HA, Frisbie CD, Whitesides GM. *Science* 1993; **260**: 647.

159 Biebuyck HA, Whitesides GM. *Langmuir* 1994; **10**: 2790.
160 Wilbur JL, Biebuyck HA, MacDonald JC, Whitesides GM. *Langmuir* 1995; **11**: 825.
161 Chaudhury MK, Whitesides GM. *Langmuir* 1991; **7**: 1013.
162 Jackman RJ, Wilbur JL, Whitesides GM. *Science* 1995; **269**: 664.
163 Bain CD, Whitesides GM. *Langmuir* 1989; **5**: 1370.
164 Hare EF, Zisman WA. *J Phys Chem* 1955; **59**: 335.
165 de Gennes P-G. *Rev Mod Phys* 1985; **57**: 827.
166 Holmes-Farley SR, Reamey RH, McCarthy TJ, Deutch J, Whitesides GM. *Langmuir* 1985; **1**: 725.
167 Biebuyck HA, Whitesides GM. *Langmuir* 1994; **10**: 4581.
168 Wilbur JL, Kim E, Xia Y, Whitesides GM. *Adv Mater*, in press.
169 Xia Y, Whitesides GM. *Adv Mater* 1995; **7**: 471.
170 Xia Y, Whitesides GM. *J Am Chem Soc* 1995; **117**: 3274.
171 Xia Y, Kim E, Mrksich M. *Chem Mater*, submitted.
172 Xia Y, Kim E, Whitesides GM. *J Electrochem Soc*, submitted.
173 Xia Y, Mrksich M, Kim E, Whitesides GM. *Langmuir*, in press.
174 Wilbur JL, Kumar A, Kim E, Whitesides GM. *Adv Mater*, 1994; **7–8**: 600.
175 Hidber PC, Helbig W, Kim E, Whitesides GM. *Langmuir*, submitted.
176 Kumar A, Biebuyck HA, Abbott NL, Whitesides GM. *J Am Chem Soc* 1992; **114**: 9188.
177 Kim E, Kumar A, Whitesides GM. *J Electrochem Soc* 1995; **142**: 628.
178 Whidden TK, Ferry DK, Kozicki MN *et al. Nanotechnology* 1994; in press.
179 Berggren KK, Bard A, Wilbur JL *et al. Science* 1995; **269**: 1255.
180 Gorman CB, Biebuyck HA, Whitesides GM. *Chem Mater* 1995; **7**: 526.
181 Potochnik SJ, Hsu DSY, Calvert JM, Pehrsson PE. *Mater Res Soc Symp Proc: Advanced Metallization for Devices and Circuits: Science, Technology and Manufacturability* 1994; **337**: 429.
182 Potochnik SJ, Pehrsson PE, Hsu DSY, Calvert JM. *Langmuir* 1995; **11**: 1841.
183 Jeon NL, Nuzzo RG, Xia Y, Mrksich M, Whitesides GM. *Langmuir*, in press.
184 Kumar A, Whitesides GM. *Science* 1994; **263**: 60.
185 Kim E, Whitesides GM, Lee LK, Smith SP, Prentiss M. *Adv Mater* 1995; in press.
186 Gorman CB, Biebuyck HA, Whitesides GM. *Chem Mater* 1995; **7**: 252.
187 Kim E, Xia Y, Whitesides GM. *Nature* 1995; **376**: 581.
188 Reiss H. *J Chem Phys* 1951; **19**: 482.
189 Prime KL, Whitesides GM. *Science* 1991; **252**: 1164.
190 Mrksich M, Whitesides GM. *TIBTECH* 1995; **13**: 228.
191 Singhvi R, Kumar A, Lopez GP *et al. Science* 1994; **264**: 696.